East West University

Project Title

Electromagnetic properties of Graphene nanoribbon (GNR) and comparison with SWCNT and Copper

Submitted by:
Farhana Sharmin
ID: 2012-2-55-066

Project Supervisor:
M. Mofazzal Hossain, Ph.D.
Professor
Department of Electronics and Communication Engineering

Declaration

I hereby declare that I have completed project on the topic entitled "Electromagnetic properties of Graphene nanoribbon (GNR) and comparison with SWCNT and Copper" as well as prepared as research report to the department of Electronics and Communication Engineering East West university in partial fulfillment of the requirement for the degree of B.Sc. in Electronics and Telecommunication Engineering, Under the course "Research/internship (ETE 498)".

I further assert that this report in question is based on my original exertion having never been produced fully and/or partially anywhere for any requirement.

……

Farhana Sharmin
ID: 2012-2-55-066
Department of ECE
East West University

Acceptance

This research report presented to the department of electronics and communication engineering, East West University is submitted in partial fulfillment of the requirement for degree of B.Sc. in Electronics and Telecommunication Engineering, under complete supervision of the undersigned.

……

M. Mofazzal Hossain, Ph.D.
Professor
Department of Electronics and Communication Engineering

Acknowledgement

First and foremost with all my heartiest devotion I am grateful to almighty Allah for blessing me with such opportunity of learning and ability to successfully complete the task.

A special Thanks with honor to my supervisor M. Mofazzal hossain who was kind enough to allocate his valuable time to provide me with his humble guidance, motivating thought and encouragement.

.....

Farhana Sharmin
2012-2-55-066

Abstract

The need for smaller and faster electronics is increasing day by day. To achieve that, one important factor is to have interconnects that can transport high frequency signal across IC elements. With that goal in mind we have tried to find a suitable material that can be used as interconnects for high frequency circuit. A theoretical investigation is carried out for predicting electromagnetic characteristics of Graphene nano-ribbon (GNR) terahertz regime. For this we have looked into the electrical properties of GNR such as resistance, capacitance and inductance. Moreover to get the proper picture, a conventional metal (copper) and another nano-material SWCNT is used in the simulation to compare the performance and decide the better material. From our work we have seen that in the lower GHZ frequency SWCNT offers better group velocity however in higher frequency copper is a better choice.

INDEX

Contents **Page No**

Chapter 01

Introduction

Carbon is one of the most important elements for all living organisms on the earth. It is an ancient but an energetic material. Around 5000BC, charcoal was used to heat and cook food. It is also used to smelt copper and iron which are the chemical materials. Most of the organic elements are made out of carbon. The adjective of having carbon atoms bond with each other in various ways, such as planner, tetrahedral and exhibiting linear bonding arrangements, made the carbon materials as unique and fascinating[1]. Carbon materials are widely used in various industries from aerospace to chemical to nuclear. As the application of carbon material is in machinery, medical, metallurgy, automotive, environmental, and construction, so that carbon materials are ubiquitous in our daily lives.[2] Graphene nanoribbons (GNRs) have one-dimensional structures with hexagonal two-dimensional carbon lattices, which are stripes of grapheme with ultra-thin width of less than 50nm. Graphene ribbons were introduced theoretically by Mitsutaka Fujita. He proposed the edge state that is unique in the grapheme zigzag edges. He also theoretically pointed out the importance and peculiarity of nanoscale and edge shape effects in nanographene. [3]

Graphene is fundamentally a single layer of graphite; a layer of sp2 bonded carbon atoms arranged in a honeycomb (hexagonal) lattice.[4] Graphene is a hexagonal array of carbon atoms extending over two dimensions endlessly. It is an atomic sheet of the same material that carbon nanotubes and graphite are made of. Graphite is the many layers of this same material stacked on top of each other.[5]

The discovery of carbon nanotubes in 1991 helped spur researchers on to produce the first sample of grapheme in 2004. Graphene is a promising candidate for the next generation of dramatically faster and more energy-efficient electronics. However, as the scientists struggled much to fabricate the materials into ultra-narrow strips, they are successful with graphene [6]. According to Arnold, “Graphene Nano ribbons that can be grown directly on the surface of a semiconductor like germanium are more compatible with planar processing that is used in the semiconductor industry, and so there would be less of a barrier to integrating these really excellent materials into electronics in the future [6].”

Graphene is a sheet of carbon atoms which has only one atom in its thickness. It conducts electrically and dissipates heat more efficiently than silicon. To exploit the remarkable properties of graphene in semiconductor applications where current must be switched on and off, graphene nano ribbons should be less than 10nm wide which is phenomenally narrow[6].

The stability of the experimentally discovered 2D single-layer grapheme is because of the gentle crumples in the third dimension, which has been proved from the far more investigations.

Graphene has been studied as the basic building block for all the graphitic materials for more than sixty years. Because it can be wrapped into 0D bucky balls, rolled into 1D carbon nanotubes (CNT), or arranged in sheets to form 3D graphite.[7,8] The discovery of single layer graphene has led to a revolution in the research field of condensed matter physics. The exceptional electronic characteristics are the main reason of it. Excellent electronic and thermal characteristics can be seen in Graphene and it is very much similar to those of carbon nanotubes (CNT).[9,10,11] Graphene is immune to electro migration, which causes problems in copper interconnects beyond the 130 nm technology node. Graphene has the capability of sustaining current densities up to three orders of magnitude higher than that of typical copper interconnects. electrons can travel long distances in grapheme without being scattered because of a certain electronic characteristics.[12,13,14]

In this work, We have analyzed Graphene nanoribon in an electrical circuit model . And we have seen the effect of Graphene in terms of its width for its electrical properties. We have found some interesting effect for this. There is a good effect for width for the resistance. We have seen the effect in term of width for the Resistance. We have developed a simplified equation for group and phase velocity from the transmission line equation. Moreover from this equation we have analyzed the electrical properties like group and phase velocity of Graphene nano ribbon with respect to frequency. Then we have finally compared the performance of GNR with copper and SWCNT.

References

[1] Yijian Ouyang, Youngki Yoon, and Jing Guo, “Scaling Behaviors of Graphene Nanoribbon FETs: A Three Dimensional Quantum Simulation Study”,IEEE Transactions on Electron Devices, Vol. 54, pp. 2223-2231, September 2007.

[2] Y. Ouyang, Y. Yoon, J. K. Fodor, and J. Guo, “Comparison of performance limits for carbon nanoribbon and carbon nanotube transistors”, Applied Physics Letters, vol. 89, pp. 203107.1-203107.3, 2006.

[3]. https://en.wikipedia.org/wiki/Graphene_nanoribbons [Update: 04.16.2016 at 8:16AM GMT+6]

[4] http://www.graphenea.com/pages/graphene-graphite#.VxJa3jArLIU [Update : 4.16.2016 at 8:16AM GMT+6]

[5] http://mrsec.gatech.edu/epitaxial-graphene [Update : 4.16.2016 at 8:16AM GMT+6

[6] http://news.wisc.edu/discovery-in-growing-graphene-nanoribbons-could-enable-faster-more-efficient-electronics/ [Update : 4.16.2016 at 8:16AM GMT+6]

[7] Antolini, E. “Graphene as a new carbon support for low-temperature fuel cell catalysts.” *Appl. Catal. B* 123:52–68, 2012

[8] Erjun Kan, Zhenyu Li and Jinlong Yang “Graphene Nanoribbons: Geometric, Electronic, and Magnetic Properties, Physics and Applications of Graphene - Theory, Dr. Sergey Mikhailov (Ed.)”, ISBN: 978-953-307152-7, 2011 .

[9] Chen, D., Tang, L. and Li, J. “ Graphene-based materials in electrochemistry”. *Chem. Soc. Rev.* 39(8):3157–3180, 2010.

[10] Wang, Y.-J., Wilkinson, D. P. and Zhang, J. “Noncarbon support materials for polymer electrolyte membrane fuel cell electrocatalysts.” *Chem. Rev.* 111(12):7625–7651, 2011.

[11] Debe, M. K. “Electrocatalyst approaches and challenges for automotive fuel cells”. *Nature* 486(7401):43–51, 2012.

[12] Sharma, S. and Pollet, B. G. “Support materials for PEMFC and DMFC electrocatalysts—a review”. *J. Power Sources* 208:96–119, 2012.

[13] Antolini, E. “Carbon supports for low-temperature fuel cell catalysts”. *Appl. Catal.* Graphene , 2009.

[14] Geim, A. K. and Novoselov, K. S. “The rise of graphene”. *Nat. Mater.* 6(3):183–191, 2007.

Chapter 2

Graphene nanoribbon

(GNR)

2.1 History of GNR

Graphene, is defined as a monolayer of carbon atoms that are hexagonally (like honeycomb) tightly packed into a 2-D lattice. The structure of graphene can also be viewed as the fewest layer limits of graphite and graphene can be produced from graphite by completing exfoliation of graphite into monoatomic layers. Graphite is a traditional carbon material which has been widely used in our daily lives for centuries. Layered structure is one of the most typical characteristics of graphite which has been successfully utilized in many applications like including the pencil lead for writing which is the most universally familiar application of graphite. When we write using a pencil, thin graphite flakes are delaminated from the lead by the mechanical friction between graphite in the pencil lead and the paper.

In 1947, Graphene was first explored as a 2-D unit for the construction of graphite theoretically research. It was the starting point to understanding the electronic properties in three-dimensional (3-D) graphite. Almost 80 years ago there were a theoretically prediction that strictly 2_D crystal cannot exist because the thermal fluctuation would destroy long-range order, giving rise to the melt of 2-D lattices. The experimental research of producing 2-D material more over Graphene has been interrupted. Early attempt to isolate grapheme sheets from graphite was conducted by using ghraphite intercalated compounds as the raw materials, since intercalation of heteroatom of molecules between Graphene layers in graphite can effective reduce the interaction. It also expand interlayer distance. Thin graphite was also prepared starting with graphite oxide in an oxidized sate of graphite. It was discovered that ultrathin carbon films could be obtained by heating or by reduction of graphite oxide in alkaline suspension. The reference paper reported the ultra-small thickness of 0.4-2nm for exfoliated sheets by analyzing the contrast of the samples in transmission electron microscopy (TEM) images corresponding to mono- and few-layer samples [1].

A few decades ago, Single- or few-layer graphene has been epitaxially grown by using gaseous carbonaceous precursors on certain substrates or thermal come attached the paper to form writing traces. There is no doubt that monoatomic layer delamination can occur during this process though the possibility may be extremely low. Therefore, it can be speculated that graphene may have already been produced centuries ago by anyone who used a pencil to write or draw, but it has never been realized and taken into serious consideration until the twentieth century. Decomposition of silicon carbide (SiC) and it has high crystallinity and high

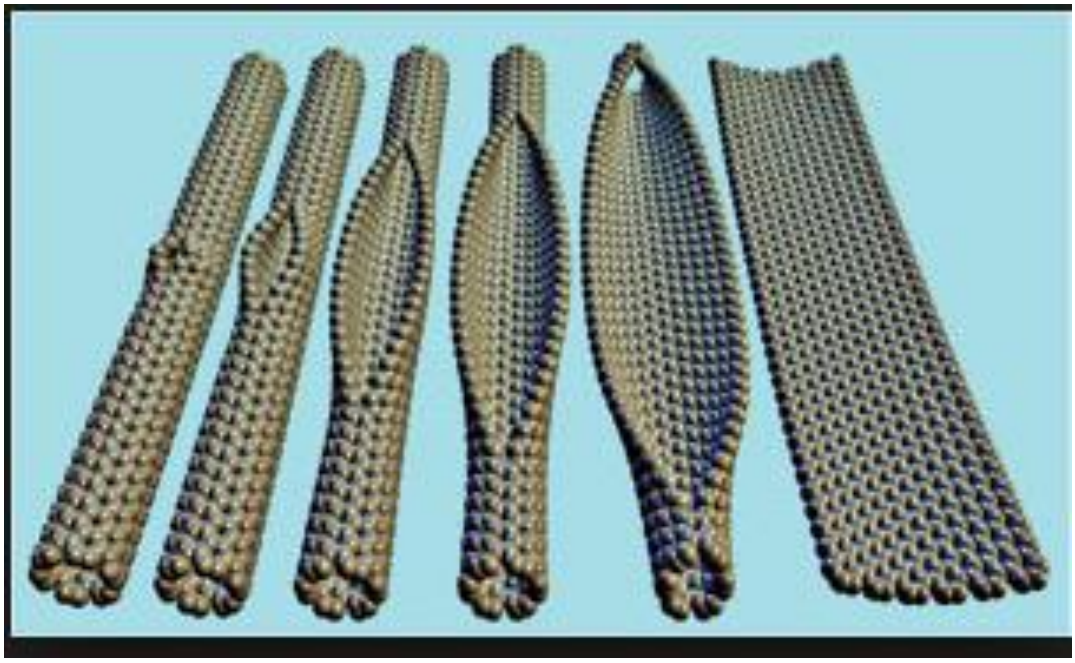

Figure 2.1: Graphene Nano-Ribbon (GNR)

Mobility charge carriers[2]. There is a strong interaction between graphene and the substrate which significantly alters the electronics structure of graphene. The measured electronic properties of graphene on the substrate may not truly reflect the properties of intrinsic graphene in a free-standing state because of this reason.

Novoselov and their research group that the curtain of the broad stage for this magic carbon material was finally drawn until the 2004 publication of pioneering work of Geim. Their experiments were quite simple. Its principle of the experiment is the mechanical exfoliation of graphite, which is actually analogous to the writing on a paper using a pencil but in a more controllable way. By repeating cleavage of graphite using common Scotch tape, the exfoliation process was realized. Ultrathin graphene sheets were finally produced with great patience. One of the secrets to their success is the usage of a silicon (Si) wafer with a 300-nm-thick silicon dioxide (SiO_2) layer on top as the substrate to load exfoliated thin graphite flakes. Such a substrate makes it possible to distinguish ultrathin graphitic layers simply by using optical observation, which enormously enhances the efficiency of the search for graphene. The as-prepared graphene is perfect in structure with almost no defects, and therefore it is possible to experimentally measure the intrinsic properties of graphene for the first time. The unique electronic properties of graphene astonished scientists, and soon significant attention was focused on this magic new carbon material all over the world. Due to their remarkable and

pioneering research work, the Nobel Prize in Physics 2010 was jointly awarded to Geim and Novoselov for “groundbreaking experiments regarding the two dimensional material graphene”[3]. Till today, tens of thousands of research papers have been published and also thousands of patents have been applied based on the materials and techniques related to graphene. Scientists believe that graphene may become a revolutionary new material which will change the world in the near future by its special properties.

2.2 Types of GNR

There are two types of Graphene Nano-Ribon on earth. They are : zig-zag and armchair. According to the characteristic appearance on the atomic scale, they are named as armchair and zig-zag.

2.2.1 Zig-zag GNR

Zig-zag GNR is emphasized by solid circles on each side of a graphene. Perpendicular to the direction of defined width, GNRs repeat their geometric structures and form one-dimensional periodic structures. As GNRs are stripes of graphene, the edge atoms are not saturated. Therefore, active edge states become an important factor to determine the edge structures. For zigzag GNRs, it was unexpectedly found that the zigzag edge is metastable and reconstruction spontaneously takes place at high temperature. The width of zigzag GNR plays an important role. The electronic properties of zigzag graphene nanoribbons (Z-GNRs) adsorbed on Si substrate strongly depending on the width of the ribbon.

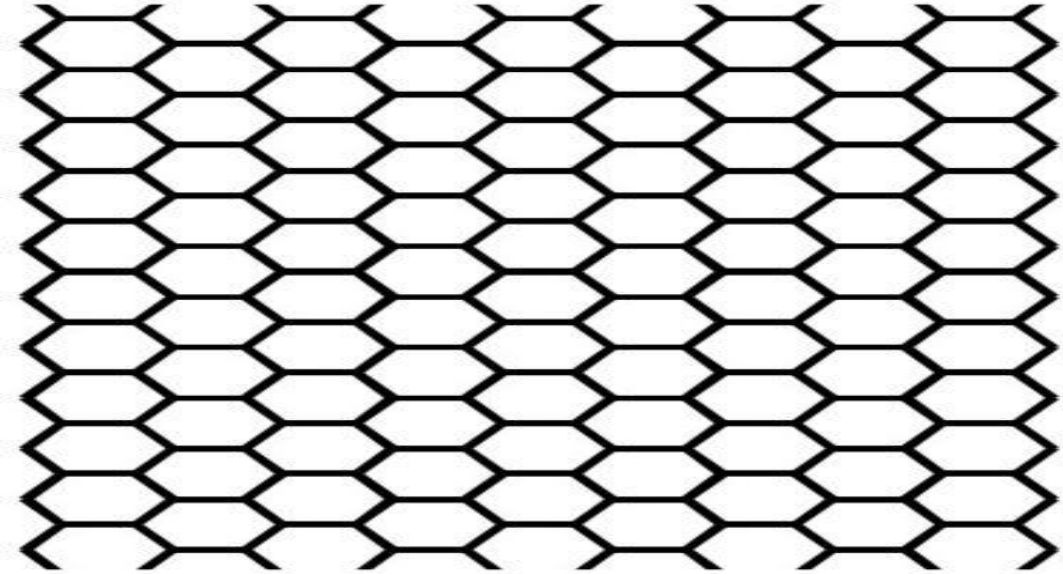

Figure 2.2: Zig-zag Graphene nanoribbon

The width of a zigzag ribbon is now identified with the number of zigzag chains N [19], $W_{zz}= (N-1)(\sqrt{3}/2)a$ With a = 1.42Å nearest neighbor distance.

The electrical conductance of zigzag graphene nanoribbons (ZGNRs) is numerically investigated in the presence of different percentages of edge and middle vacancies. The vacancies are randomly distributed in the edge or innermost of ZGNRs. We take advantage of recursive Green's function under tight-binding model to study the electrical conductance. It is found that in the both vacancy types, and all widths and lengths of our samples, the conductance degrades as the vacancy concentration increases. In addition, we illustrate how transport properties are sensitive to the width and length of nanoribbon. At fixed defect concentration, the length growth leads to exponential decrease, and the width growth leads to power law increase in the conductance of ZGNRs, respectively. Under the same numerical framework, we have also studied transition from metal to insulator and vice versa .

2.2.1.1 Electron Transport in Zigzag GNR

Zigzag-edged single and double folded graphene nanoribbons are studied using density functional theory methods. Some asymmetric folds and folds with an octagon/hexagonal extended defect line are also considered. The long-range van der Waals interactions are taken into account *via* semiempirical pairwise optimized potential. The geometrical and magnetic phases of the studied structures are obtained. It is shown that the magnetic states of the folds depend strongly on their stacking patterns. The electronic structures in terms of energy needed for the folding process, van der Waals contribution, energy band gaps, band structures, and densities of states are also calculated.

Depending on the graphene's edge shape and width , a finite width has been shown to hold unusual electronic properties .Depending on these earlier studies ,all zigzag GNRs (ZGNRs) were predicted to be metallic while AGNRs were grouped into semiconducting and metallic character. The metallic character of ZGNRs was attributed to the presence of a high density of edge states at the Fermi level. The zigzag edges present electronic localized states at the boundaries, corresponding to non-bonding states that appear at the Fermi level as a large peak in the density of states. Phenomena related to magnetic and spin properties arising due to specific edge structure of graphene ribbons have also been investigated theoretically. Due to the non-bonding character of the zigzag localized edge states, the geometrical reconstruction is unlikely to happen and the spin polarization of the electronic density establishes an anti-ferromagnetic arrangement (Figure 2.3) with the opening of a gap, yielding a Slater insulator [4] .

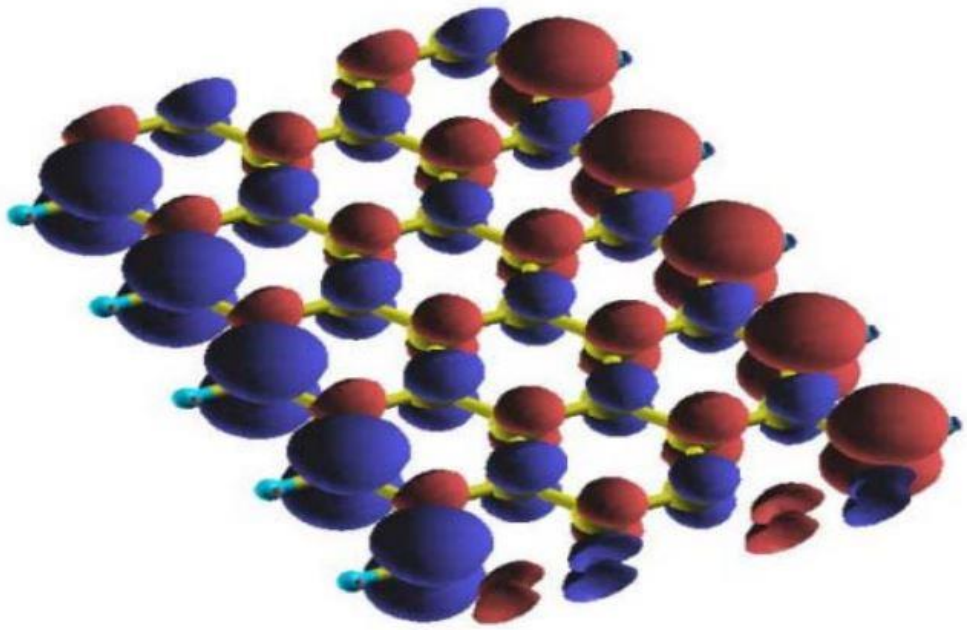

Figure 2.3: Spin density map, showing the anti-ferromagnetic arrangement between opposite edges (Ricardo F et al., 2009 [5]).

In details, graphene nanoribbons with zigzag edges (ZGNRs) possess spin polarized peculiar edge states and spin polarized electronic state provides half metallicity under transverse electric field and has great potential in the application as spintronics. It is mainly attributed that an in plane electric field, perpendicular to the periodic axis, induces a half metal state in zigzag nanoribbons (ZGNR). Apart from the interesting dependence of the electronic structure upon an electric field, this is a promising material for future spintronic devices, since it could work as a perfect spin filter.

2.2.2 Armchair GNR

The edge sites are emphasized by solid circles on each side. Perpendicular to the direction of defined width, GNRs repeat their geometric structures, and form one-dimensional periodic structures. Since GNRs are stripes of graphene, edge atoms are not saturated. Therefore, active edge states become an important factor to determine the edge structures. For armchair GNRs (figure 2.4), there is no edge reconstruction, and the planar patterns are kept.

Wac=(N-1)((³^.5/2)a With a = 1.42Å nearest neighbor distance

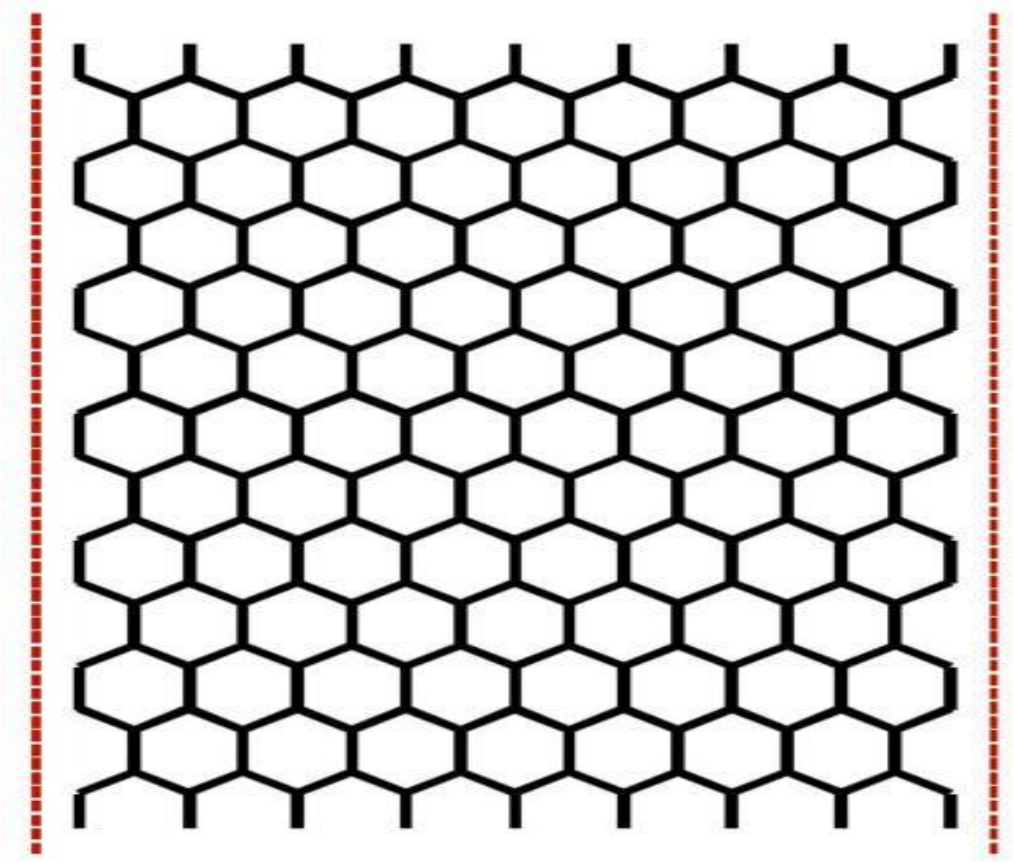

Figure 2.4: Armchair graphene Nano-Ribon

The width of an armchair ribbon can be defined in terms of the number of dimer lines [6]

2.2.2.1 Electron Transport in Armchair GNR

Many theoretical studies have been devoted into investigating the electronic properties of armchair GNRs, such as tight-binding calculations, density functional theory (DFT) calculations, and many-electron green‘s function approach. Among those methods, DFT calculations adopt parameter free self-consistent field calculations, and their reliability has been broadly proved in solid state field and nano-scale systems. Thus, most of the theoretical investigations have been carried out with DFT calculations. However, it is well established that DFT calculations underestimate band gaps. Other methods, such as tight-binding calculations, have been adapted to correct DFT calculations, and get the reliable band gaps. Armchair GNRs show

semiconducting behaviors with a direct energy gap. The determining factor comes from the quantum confinement effect (QCE), which can be characterized by energy gaps is inverse of width. Besides the QCE, researchers have pointed that the edge effects play an important role to force the armchair GNRs to be semiconductors. As shown in figure 2.4, the edge of carbon atoms of armchair GNRs are usually passivated by hydrogen atoms, which lead to the bonding of carbon atoms at the edges different with other carbon atoms. As a consequence, the bond lengths of carbon atoms at the edges are shorter than that in the middle of ribbons, and open the energy gaps of armchair GNRs. Although armchair GNRs have three typical families (corresponding to N = 3p, 3p+1, 3p+2, respectively, where p is any integer) with distinguished energy gaps, they have similar band shapes [7].

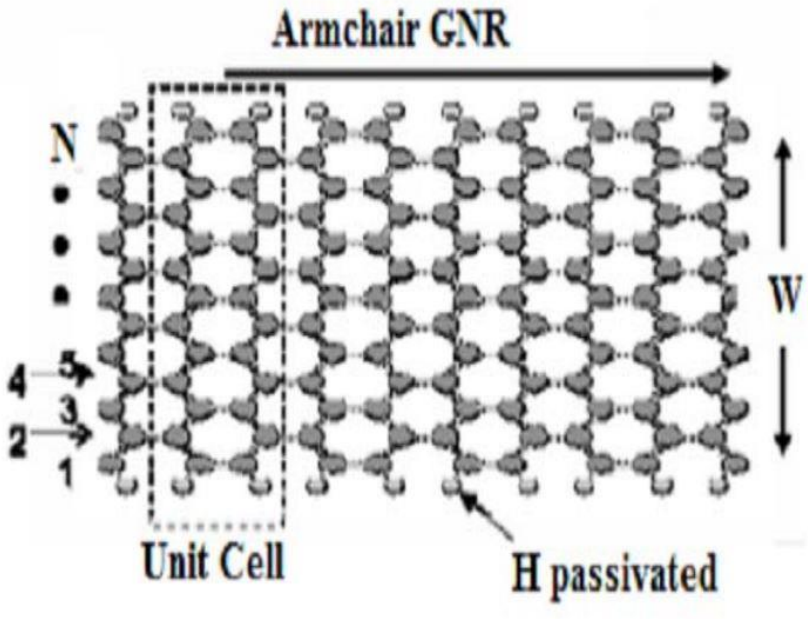

Figure 2.5: Atomic structure of armchair Graphene Nano-Ribon [8]

2.3 Properties

Properties of Graphene nano-Ribon are quite different that the material we generally use. These properties made GNRs such important materials for using in Nano technology. Some properties are discussed below in general.

2.3.1 Electronic properties

The high quality of 2-D crystal lattice endows graphene with extraordinary electronic properties. The valence and conduction bands in graphene intersect at a single point of zero states, which is called the Dirac point, which makes graphene a zero-gap semiconductor. At the Dirac point, the density of states is zero and the linear dispersion relation results in an effective mass of zero. Therefore, electrons in graphene behave as massless Dirac fermions, giving rise to unprecedentedly high carrier mobility. The carrier mobility measured for a high-quality single-layer graphene sheet prepared by mechanical exfoliation and completely suspended with no influence of the substrate reaches 200,000 cm2 V–1 s–1. With such high-carrier mobility, the charge transport in graphene is actually ballistic on the micrometer scale at room temperature. The charge carriers in graphene behave like relativistic particles. As a result, their behavior should be described using the Dirac equation instead of the Schrodinger equation, generally applied to describe the electronic properties of other materials. Therefore, the emerge of graphene now provides scientists with the possibility to investigate relativity theory on the lab table instead of in the universe, and provides a way to study quantum electrodynamics by measuring graphene's electronic properties. Another characteristic of graphene is its ambipolar electric field effect. The carriers in graphene can be continuously tuned between holes and electrons by supplying the requisite gate bias. This means that under negative gate bias, the Fermi level drops below the Dirac point, giving rise to a large population of holes in the valence band, while under positive gate bias, the Fermi level was raised above the Dirac point, introducing a large population of electrons in the conduction band. The mobility of charge carriers can exceed 15,000 cm2 V–1 s–1 even when their concentration is as high as 1013 cm–2 at ambient conditions [9,10] and the observed mobility is weakly dependent on temperature. Due to the atomically thin structure of graphene, electron transport on graphene is strictly confined in the 2-D plane, which creates a so-called 2-D electron gas and induces some unique phenomena, such as a quantum Hall effect even observed at room temperature. Klein tunneling is another feature of graphene, which is derived from the chiral nature of electron transport in graphene. This means that the electrons in graphene have a 100% transmission rate through a potential barrier of any size. This may bring about some difficulties in manipulating graphene-based devices, as square potential barriers usually applied to form the device channel may be ineffective for graphene. The intrinsic electronic properties of graphene have been extensively studied and will cause not much excitement on their own. However, the interference of graphene with intrinsic or extrinsic scatters, such as doping atoms or substrates, will cause novel transport phenomena, which is a useful way to tune the electron properties of graphene to meet different application purposes.

2.3.2 Optical properties

About 97.7% of a single layer has been experimentally observed in the visible range for a constant transparency, which means that atomic monolayer graphene has an unexpectedly high opacity, absorbing $\pi\alpha \approx 2.3\%$ of white light, where α is the finestructure constant [11]. This is a consequence of the unusual low-energy electronic structure of monolayer graphene that features electron and hole conical bands meeting each other at the Dirac point. It is noteworthy that the transmittance decreases linearly with the number of layers for multilayer graphene [12], so that the thickness of multilayer graphene with less than 10 layers can be determined using white light illumination on samples supported on a given substrate. However, if the thickness of graphene increases to more than 10 layers, the optical property eventually becomes more like that of graphite. Based on the Slonczewski–Weiss–McClure band model of graphite, the interatomic distance, hopping value, and frequency cancel when optical conductance is calculated using Fresnel equations in the thin-film limit. That is to say, thick graphene platelets with tens of layers will never share the same optical property with the monolayer one.

Considering the real application for a graphene-based Bragg grating, which is a one-dimensional photonic crystal, has been fabricated and demonstrated its capability for excitation of surface electromagnetic waves in the periodic structure by using a 633-nm helium–neon (He–Ne) laser as the light source.

2.3.3 Thermal properties

Single-layer graphene has the highest intrinsic thermal conductivity that has ever been found in any material. As high as 6000 W m–1 K–1 [13], the intrinsic thermal conductivity of graphene is even higher than its allotrope-carbon nanotube, which is 3500 W m–1 K–1 [14,15], and certainly higher than those metals with good thermal performance, such as gold, silver, copper, and aluminum. This excellent thermal performance is born from the unique electronic and topographic features of graphene. However, according to [16], placing graphene on substrates results in serious degradation of thermal conductivity to 600 W mK–1, lower than values obtained for suspended graphene. Since the carrier density of nondoped graphene is relatively low, the electronic contribution to thermal conductivity is negligible according to the Wiedemann–Franz law [17]. The thermal conductivity of graphene is thus dominated by phonon transport, namely diffusive conduction at high temperature and ballistic conduction at sufficiently low temperature. Now we can say that the degradation of thermal conductivity is owing to the phonons leaking across the graphene-support interface and strong interface scattering of flexural modes. In any case, due to the extraordinary thermal conductivity of graphene, graphene functionalized nanocomposites have been studied for various advanced

applications including thermal management of advanced electronic chips, thermal pastes, and smart polymers.

2.3.4 Mechanical Properties

Graphene is mechanically strong while remaining very flexible, which is attributed to the high strength of the carbon–carbon bond. The elastic properties and intrinsic breaking strength of free-standing monolayer graphene were measured by nanoindentation using an atomic-force microscopy [18]. The experimental data showed that the mechanical properties of graphene measured in experiments have exceeded those obtained in any other material, with some reaching theoretically predicted limits that were investigated by numerical simulations such as molecular dynamics [19]. For example, a single-layer, defect-free graphene was measured with a Young's modulus of 1 TPa and intrinsic fracture strength of 130 GPa. These high values make graphene very strong and rigid and these incredible mechanical performances are benefited from the hexagonal structure of graphene. Interestingly, despite sharing the same honeycomb lattice, bulk graphite is not particularly strong because it shears very easily between layers. As a derivative of graphene, GO in a paper form was prepared and studied as a ramification of graphene. The average elastic modulus and the highest fracture strength obtained were about 32 GPa and 120 MPa, respectively [20]. The decrease of Young's modulus may be caused by the defects introduced during the chemical reaction. After reduction with hydrazine or annealing, a paper composed of stacked and overlapped graphene platelets was obtained and the stiffness and tensile strength were reinforced [21]. Chemically modified graphene obtained by reducing GO with hydrogen plasma exhibited a mean elastic modulus of 0.25 TPa with a standard deviation of 0.15 TPa. Just as the Nobel announcement said, a 1-square-meter graphene hammock would support a 4-kg cat, but would weigh only as much as one of the cat's whiskers at 0.77 mg, which is about 0.001% of the weight of 1 m2 of paper. These outstanding intrinsic mechanical properties make graphene suitable for diverse applications such as pressure sensors, resonators, and engineering components subjected to large mechanical stresses even under extreme conditions.

2.3.5 Magnetic Transport Properties of Graphene nanoribbons

Theoretical investigations are done on spintronics and magnetic device properties of STGNRs. The typical properties of bipolar magnetic semiconductors are featured by the STGNRs at a FM ground state. Compared to ZGNRs their Curie temperature T is much higher. A very significant fact is that the dual spin filtering effect with the perfect spin polarization and high performance dual spin diode effect with a rectification ratio about 10^{10} can be achieved. This is a much greater value as compared to that for a ZGNR diode (~10^{5}~) and macroscopic p-n junction diodes (10^{5}~ 10^{7}). A giant magnetoresistace approaching 10^{10}% displayed by a highly effective spin valve device is three orders magnitude higher than the value predicted based on the ZGNRs and six

orders magnitude higher than previously reported experimental values for the MgO tunnel junction. These idiosyncratic features can be endorsed to their unique band overlap pattern for two electrodes and particular sensitivity to a switching magnetic field. For developing STDs, the research suggests that STGGNRs have a promising performance.

For edge carbon atoms of GNRs there exists two types of hybridizations, sp^2 and sp^3 hybridizations. The usual edge structure under a lower hydrogen-concentration is generally regarded as the sp^2 hybridized mono hydrogen termination. That is why, in most of the literatures mono hydrogen terminated structures fog nr are presented and investigated. This type of termination for STGNRs is still being searched. Edge structure of GNR is usually diversified, for example di-hydrogen termination, edge reconstruction, Z, passivate edge, edge defects and other chemical modifications. These might have an impact on magnetism. Further works will deal with this complicated cases. It is quite difficult to achieve the required atomic precision for fabricating StGNRs in the current experiments, but theoretical modeling to understand the magnetic structure and magnetic transport properties of ideal STGNRs is very much significant.

Exchange correlation functionals for DFT used in our works might underestimate the band gap of AGNRs compared with other algorithms. The GW method is one of its example. If other more exact methods are used for calculations there would be a larger spin splitting energy gap E.Spin splitting energy gap is really well related with the spin polarization and spin diode effect as well as the spin valve device.

2.3.6 Non-Linear properties

Linear elastic behavior of all GNRs are being displayed from the nominal stress-strain curves in Fig-2. Following that the linear regimes of the GNRs can be written as b e E W E0 E0 0 3 = +, [21].

Here b E0 is the initial young modulus of the bulk grapheme and e E0 is the initial edge modulus. The bulk graphene is isotropic in the regime of linear elasticity and the edge modulus depends on the edge chirality with different values for the zigzag and armchair edges. As it is shown in Fig. 3, the initial Young's modulus of the GNR depends on the edge chirality and the ribbon width. present studies after using the REBO potential express their views that a bulk Young Modulusm 243 0=b E N/mm and the predicted edge modulus is 8.33 0= e E nN (52 eV/nm) for the unpassivated zigzag edge and =3.65 e E nN (~22.8 eV/nm) for the unpassivated armchair edge. The Young mdulus among positive moduli for both edges, the GNR increases as the ribbon width decreases. The predicted edge modulus, which was predicted earlier, is considerably lower than a previous calculation using a different potential and the REBO potential is known to underestimate the bulk modulus. Initial Young modulus against the ribbon width for GNRs with unpassivated and hydrogen-passivated edges. The potential energy in Eq. (1) is modified account for the hydrogen adsorption, which has passivated edges.

H is the adsorption energy of Hydrigen per unit length along the edges of the GNR. The negative signs indicates typically reduced edge energy due to hydrogen passivation. While comparing the potential energies for the GNRs with or without H passivation, the adsorption energy can be determine as a function of the nominal strain for both armchair and zigzag edges. At the level of zero strain our MM calculations predict the hydrogen adsorption energy to be 20.5 and 22.6 eV/nm for the zigzag and armchair edges, respectively, which compare closely with the first principle calculations. The adsorption energy varies under uniaxial tension and it also varies with normal strain.

A negative edge modulus (20.5 0 = − e E eV/nm) is obtained in the latter case and thus the initial Young's modulus decreases with decreasing ribbon width, opposite to the unpassivated GNRs. The horizontal dashed line in every single figure indicates the fracture strain of bulk graphene under uniaxial tension in the same direction. the bulk graphene fractures without any defect when the tangent modulus becomes zero (i.e., / 0 2 2 d U dε =), dictated by the intrinsic lattice instability under tension.

Fracture may occur much earlier due to thermally activated processes at a finite temperature. the critical strain to fracture for bulk graphene varies with the loading direction which was shown in an earlier study. first-principle calculations [22, 23] and empirical potential models both have predicted that the intrinsic critical strain is higher for graphene under uniaxial tension in the zigzag direction than in the armchair direction, suggesting that the hexagonal lattice of graphene preferably fractures along the zigzag directions by cleavage.

The GNRs with zigzag edges fracture at a critical strain close to that of bulk graphene loaded in the same direction as it is shown in Fig 1a. Fig. 1b shows a very contrastive way that the GNRs with armchair edges fracture at a critical (a) (b) strain considerably lower than bulk graphene. As shown in Fig 4, the fracture strain slightly depends on the ribbon width in both cases. The process of Hydrogen passivation of the edges leads to slightly lower fracture strains for zigzag GNRs, but slightly higher fracture strains for armchair GNRs. different fracture mechanisms for the zigzag and armchair GNRs are implied by the apparently different edge effects on the fracture strain. at different temperatures the processes of fracture nucleation in GNRs are studied by molecular dynamics (MD) simulations. Studies have proven that the edge effect leads to two distinct mechanisms for fracture nucleation in GNRs at relatively low temperatures (T < 300 K). Two fractured GNRs at 50 K are showen by the Fif 5. Fracture nucleation occurs stochastically at the interior lattice of the zigzag GNRs. For this very reason the fracture strain is very close to that of bulk graphene strained in the same direction, consistent with the MM calculations. For the GNR with armchair edges (Fig. 5b), fracture nucleation occurs most often near the edges. Leading to a lower fracture strain compared to bulk graphene, as seen also from the MM calculations, the armchair edge serves as the preferred location for fracture nucleation.

The same mechanisms hold for GNRs with H-passivated edges. Evidences of Fig 5 prove that that cracks preferably grow along the zigzag directions of the graphene lattice in both cases.

References

[1] Y. Ouyang, Y. Yoon, J. K. Fodor, and J. Guo, "Comparison of performance limits for carbon nanoribbon and carbon nanotube transistors", Applied Physics Letters, vol. 89, pp. 203107.1-203107.3, 2006.

[2] Pavel B. Sorokin, Pavel V. Avramov, Viktor A. Demin, Keonid A. Shernozatonskii, "Metallic Beta-Phase Silicon Nanowires:Structure and Electronic Properties",vol.1,13 Jun 2009.

[3] Jeroen W. G. Wilder, Liesbeth C. Venema, Andrew G. Rinzler, Richard E. Smalley & Cees Dekker, "Electronic structure of atomically resolved carbon nanotubes", Nature, Vol. 391, pp. 59, Jan 1998.

[4] Li, X., Cai, W., An, J. et al. "Large-area synthesis of high-quality and uniform graphene films on copper foils". *Science* 324:1312–1314, 2009.

[5] Wu, W., Jauregui, L. A., Su, Z. et al. "Growth of single crystal graphene arrays by locally controlling nucleation on polycrystalline Cu using chemical vapor deposition". *Adv. Mater*,2011.

[6] Jeroen W. G. Wilder, Liesbeth C. Venema, Andrew G. Rinzler, Richard E. Smalley & Cees Dekker, "Electronic structure of atomically resolved carbon nanotubes", Nature, Vol. 391, pp. 59, Jan 1998.

[7] Mceuen, P.L. Lab. Of Atomic & Solid State Phys., Cornell Univ., Ithaca, NY Fuhrer, M.S. ; Hongkun Park, "Single-Walled Carbon Nanotube Electronics",Vol. 1,Issue: 1, pp. 78-85, Mar 2002

[8] G. Liang (NUS), Neophytos Neophytou (Purdue), Mark S. Lundstrom (Purdue), Dmitri Nikonov (Intel) , "Theoretical study of graphene nanoribbon field-effect transistors", 887.016 (Purdue University), Vol. 1,pp-127 – 130, Nanotech 2007

[9] Emtsev, K. V., Bostwick, A., Horn, K. et al. "Towards wafer-size graphene layers by atmospheric pressure graphitization of silicon carbide". *Nat. Mater.* 8:203–207, 2009.

[10] Su, C.-Y., Lu, A.-Y., Wu, C.-Y. et al. " Direct formation of wafer scale graphene thin layers on insulating substrates by chemical vapor deposition". *Nano Lett*. 11:3612–3616, 2011.

[11] Kholmanov, I. N., Magnuson, C. W., Aliev, A. E. et al. "Improved electrical conductivity of graphene films integrated with metal nanowires". *Nano Lett.* 12:5679–5683, 2012.

[12] Yan, Z., Lin, J., Peng, Z. et al. "Toward the synthesis of wafer-scale single-crystal graphene on copper foils". *ACS Nano* 6:9110–9117, 2012.

[13] Huang, P. Y., Ruiz-Vargas, C. S., van der Zande, A. M. et al. 2011. Grains and grain boundaries in single-layer graphene atomic patchwork quilts. *Nature* 469:389–392.

[14] Yamada, T., Kim, J., Ishihara, M. et al. "Low-temperature graphene synthesis using microwave plasma CVD". *J. Phys. D: Appl. Phys.* 46:063001, 2013.

[15] Geng, D., Wu, B., Guo, Y. et al. "Uniform hexagonal graphene flakes and films

grown on liquid copper surface". *Proc. Natl. Acad. Sci. U.S.A.* 109:7992–7996, 2012.
[16] Vlassiouk, I., Smirnov, S., Regmi, M. et al. "Graphene nucleation density on copper: Fundamental role of background pressure". *J. Phys. Chem. C* 117:18919–18926, 2013.
[17] Chen, S., Ji, H., Chou, H. et al. "Millimeter-size single-crystal graphene by suppressing evaporative loss of Cu during low pressure chemical vapor deposition." *Adv. Mater.* 25:2062–2065,2013.
[18] Wu, B., Geng, D., Guo, Y. et al. "Equiangular hexagon-shape-controlled synthesis of graphene on copper surface." *Adv. Mater.* 23:3522–3525, 2011.
[19] Jacobberger, R. M. and Arnold, M. S. "Graphene growth dynamics on epitaxial copper thin films. *Chem. Mater"* 25:871–877, 2009
[20] Sun, Z., Yan, Z., Yao, J. et al."Growth of graphene from solid carbon sources." *Nature* 468:549–552, 2010
23:4898–4903.
[21] Ricardo Faccio, Pablo A Denis, Helena Pardo,Cecilia Goyenola ,and A lvaro WMombru, "Mechanical properties of graphene nanoribbons",J. Phys.: Condens.Matter, vol. 21, pp. 285304-285311, 2009
[22] Kwon, S.-Y., Ciobanu, C. V., Petrova, V. et al. "Growth of semiconducting graphene on palladium." *Nano Lett.* 9:3985–3990, 2009.
[23] Ramón, M. E., Gupta, A., Corbet, C. et al. "CMOS-compatible synthesis of largearea, high-mobility graphene by chemical vapor deposition of acetylene on cobalt thin films." *ACS Nano* 5:7198–7204, 2011

Chapter 03

Electromagnetic Properties of Graphene nanoribbon

To see the effect of conductance for Graphene Nano-Ribbon, we took a RLC circuit model with GNR interconnect. We got some equation from there. Which help us to saw the conductance effect of GNR.

There are two terminals named as P and N. P represent positive and N represent Negative terminal of a GNR interconnect. This circuit is a distributed RLC equivalent circuit for GNRs which considered in the model. In this model there are few parameter:

R_Q represent the quantum contract resistance.

R represent the GNR resistance per unit length.

I_M Represent magnetic inductance per unit length of GNR.

I_K represent the kinetic inductance per unit length of GNR.

C_Q and **C_E** are the GNR quantum capacitance and electrostatic capacitance per unit length. Also it is noticeable that terminal **P** and **N** are symmetric, completely interchangeable.

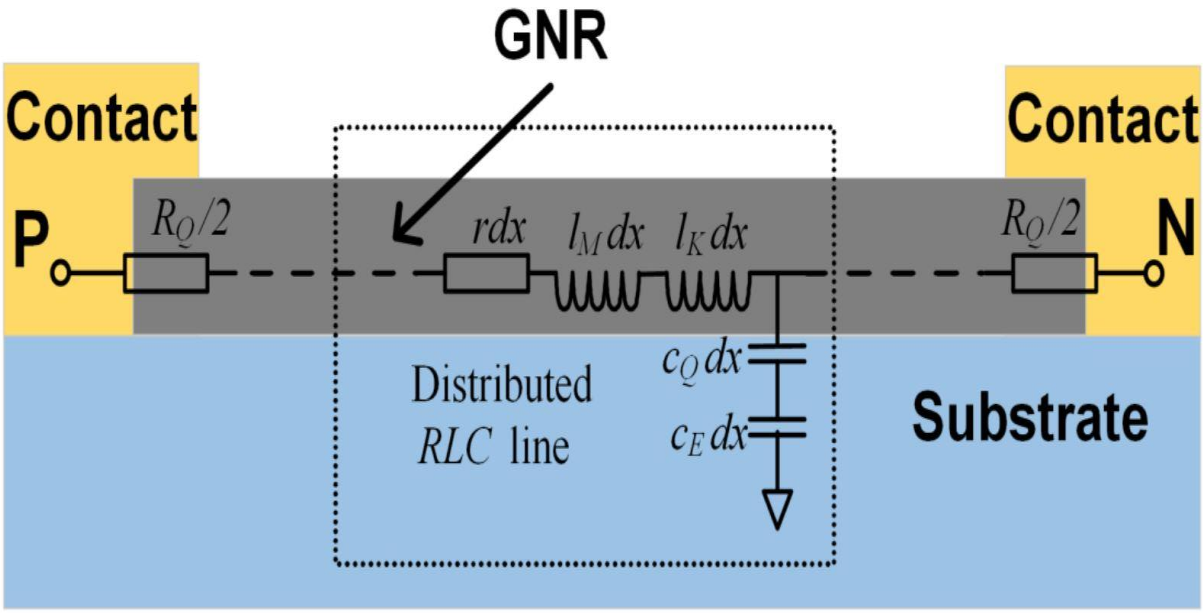

Figure 3.1: Schematic of a GNR interconnect and corresponding RLC distributed circuit model [1]

3.1 GNR Resistance

Total resistance of GNR is the combination of quantum capacitance and total resistance for a single GNR layer's total conductance which is the summation of conductance of electrons and holes.

Now, The quantum contact resistance (R_Q) of GNR is can be written as:

$R_Q = h /(N_{ch} . N_{layer}. 2q^2)$ ……(3.1)

Where h= plank's constant;

q= charge of electrons;

N_{ch}= number of conducting channel mode of GNR;

N_{layer}= number of layer of GNR.

For simplification we have considered $N_{ch} = 1$ and $N_{layer} = 2$.

Again the total conductance of a single layer GNR is :

$G_{total} = \sum_n G_n$ (electrons) + $\sum_n G_n$ (holes) ……(3.2)

Where Gn is the conductance of the nth conduction mode, can be expressed for a single layer GNR depending on the linear response Laudauer formula is :

$G_n = \frac{2q^2}{h} \int T_n(E) \left(-\frac{\partial f_0}{\partial E}\right) dE$ ……..(3.3)

Here $f_0 (E) = \{1 + \exp [(E-E_F)/ k_B T] \}^{-1}$ ……(3.4)

Here,
$T_n(E)$ represents the transmission coefficient,

$f_0(E)$ represents the Fermi-Dirac distribution function.

E_F is the Fermi level.

k_B is the Boltzmann's constant.

T represent the temperature.

Using the Matthiessen's rule, $T_n(E)$ can be obtained by

$$\frac{1}{Tn\,(E)} = 1 + \frac{L}{l_D\,cos\theta} + \frac{L}{wcot\theta} \approx \frac{L}{l_D cos\theta} + \frac{L}{wcot\theta} \qquad \text{…….. (3.5)}$$

Here, l_D is the carrier mean free path.

w is the width of GNR.

cotθ represent the ratio of longitudinal to transverse velocities in (3.5).

Transforming equation (3.2) to integration form, we can write

$G_{total} = \frac{2}{\Delta En}\ [\int_0^{\infty} G_n\,(\text{electrons})d\,E_n + \int_{-\infty}^{0} G_n\,(\text{holes})\,dE_n]$ ……(3.6)

Deriving it, we get

$G_{total} = \frac{4q^2w^2}{Lh^2vf}\ 2k_B\ T\ \ln\ [2\cosh\ (E_F/\ 2k_BT)].\ func\ (w,l_D)$ …….. *(3.7)*

where *func*(*w*, l_D) is :

$$func(w,l_D) = \begin{cases} \frac{\pi w - 2l_D}{l_D} + \frac{4\sqrt{(l_D^2 - w^2)}}{l_D}\,.archtanh\left(\sqrt{\frac{l_D - w}{l_D + w}}\right), l_D \geq w \\ \frac{\pi w - 2\,l_D}{l_D} - \frac{4\sqrt{(l_D^2 - w^2)}}{l_D}\,.\arctan\left(\sqrt{\frac{l_D - w}{l_D + w}}\right), l_D < w \end{cases} \qquad \text{…….. (3.8)}$$

Where l_D is the mean free path ,w is the width of the GNR.

Practically l_D is 1×10^{-6} m and width is always nano-meter. So we have to consider the 2nd condition for $l_D < w$ of func(w, l_D) to get the G_{total} .

Now with the proper value of parameters, we can see the effect of change of resistance with respect to width by considering

N_{layer}=1;

N_{ch}=2;

Permittivity of free space , ε_0 =8.854*10^-12 F/m,

Permeability for free space, μ_0 =1.256*10^-6 N/A^2,

Boltzmann's constant,k_B=1.38*10^-23J/K;

Fermi level,E_f=-0.21*(1.6e-19) V;

Frequency ,f= 1e9 Hz;

Width of GNR, w= 10nm to 100nm ,

Mean free path, l_D= 1×10^-6 m ,

Plank's constant, h = 6.602 × 10 ^{34} J-s,

Fermi velocity, V_f =8*10^5 m/s;

Length of GNR, L=100*10^-9 nm;

Electron's charge, q= 1.602*10^-19C;

Temperature, T=300K.

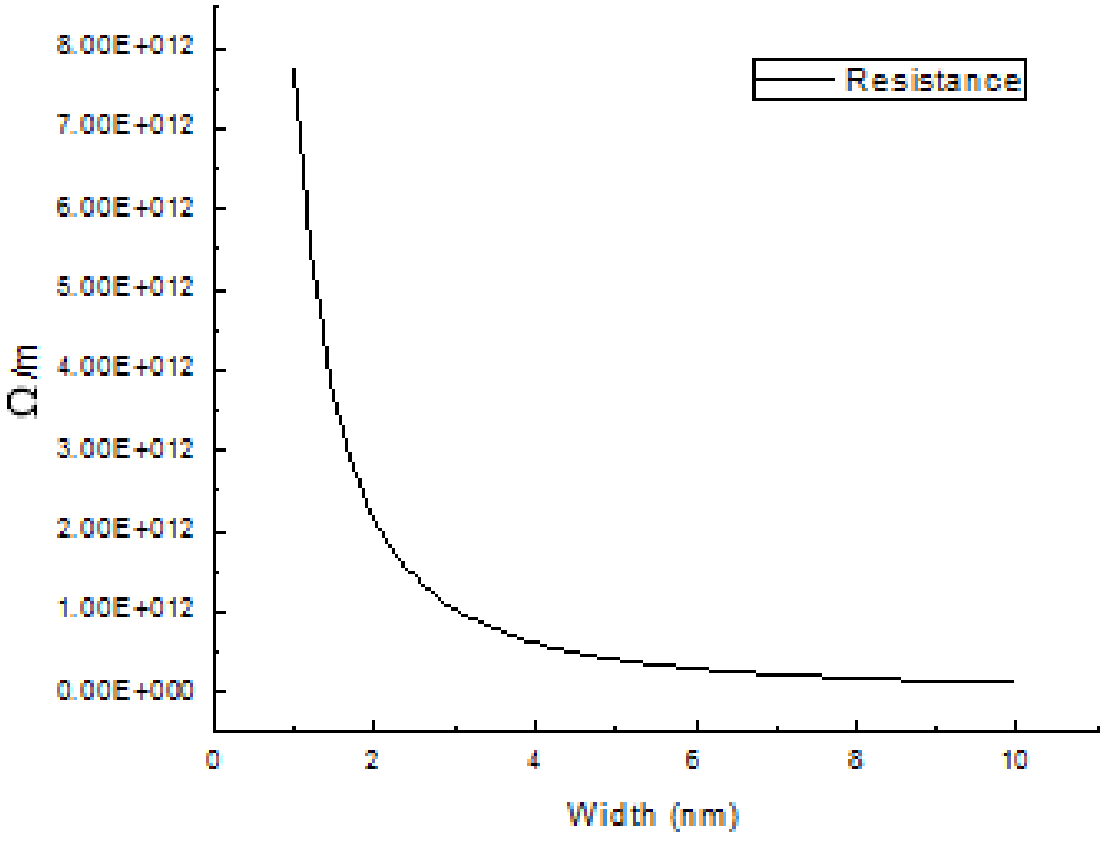

Figure 3.1 : Dependency of resistance on width of GNR for N_{ch} = 2 and N_{layer} = 1

The graph shows that resistance decreases with increasing of width of GNR which is our desired result. Because for producing a better interconnector , low resistance is an important parameter.

3.2 Capacitance of GNR

Capacitance is the ability of a body to store an electrical charge. A material with a large capacitance holds more electric charge at a given voltage than one with low capacitance [2]. As GNR is a material of small body, its capacitance will be low.

The total capacitance of GNR per unit length is calculated by the electrostatic capacitance and quantum capacitance:

$C_{total} = C_Q C_E / (C_Q + C_E)$

where

$C_Q = (N_{layer} N_{ch} 4q^2)/ hv_f$

$$= 1 \times 2 \times 4 \times \left(1.6 \times 10^{-(19)}\right)^2 \Big/ 8 \times 10^5 \times 6.602 \times 10^{-34}$$

$=3.863\times10^{-10}$ F/m

Here V_f is the Fermi velocity.

And

$C_E= (\varepsilon_0 w / d) = 2 \varepsilon_0 = 2 \times 8.854\times10^{-12} = 1.77 \times 10^{-11}$ F/m

Where d= w/2 .

So total capacitance is $C_{total} = \frac{3.863\times10^{-10}\times1.77\times10^{-11}}{3.863\times10^{-10}+1.77\times10^{-11}} =$ 1.6932×10^{-11} F/m

Here we get that the capacitance per unit length is very low.

3.3.3 Inductance of GNR

Inductance is the property of an electric conductor or circuit that causes an electromotive force to be generated by a change in the current flowing [3]. The total inductance per unit length is the summation of magnetic inductance and kinetic inductance where magnetic inductance is:

$l_M = \mu_0 (d/w) = \mu_0 /2 = \frac{1.256*10\text{^}-6}{2} = 6.283 \times 10^{-15}$ H/m .

And kinetic inductance is :

$l_K = h/ (N_{layer} . N_{ch} . 4q^2 . V_f)$

$= \frac{6.602 \times 10^{-34}}{1\times2\times4\times(1.6\times10^{-19})^2\times8\times10^5} = 4.044 \times 10^{-3}$ H/m

So, total inductance is :

$L_{total} = l_M + l_K$ ----------(3.10)

$= (6.283 \times 10^{-15}) + (4.044 \times 10^{-3}) =$ 0.0040 H/m

Reference

[1] Junkai Jiang, Jiahao Kang, Wei Cao, Chuan Xu, Prof. Kaustav Banerjee “UCSB Graphene-Nano-Ribbon (GNR) Interconnect model (VERSION = 0.9.0) ” 3/XX/2015

[2] https://en.wikipedia.org/wiki/Capacitance

[3] https://www.google.com/webhp?sourceid=chrome-instant&ion=1&espv=2&ie=UTF-8#q=definition+of+inductance

Chapter 04

Results and comparison

There are some phenomena of a graphene nano ribbon material (GNR) material when voltage is applied to it.

4.1 Attenuation

In physics, attenuation is the gradual loss in in intensity of any kind of flux through a medium.

In electrical engineering and telecommunication, attenuation affects the propagation of waves and signals in electric circuits, in optical fiber and in air. [1]

$$\alpha = \frac{1}{\sqrt{2}} \left[\sqrt{\omega^4 L^2 C^2 + \omega^2 R^2 C^2} - \omega^2 LC\right]^{\frac{1}{2}} \quad \text{..... (4.1)}$$

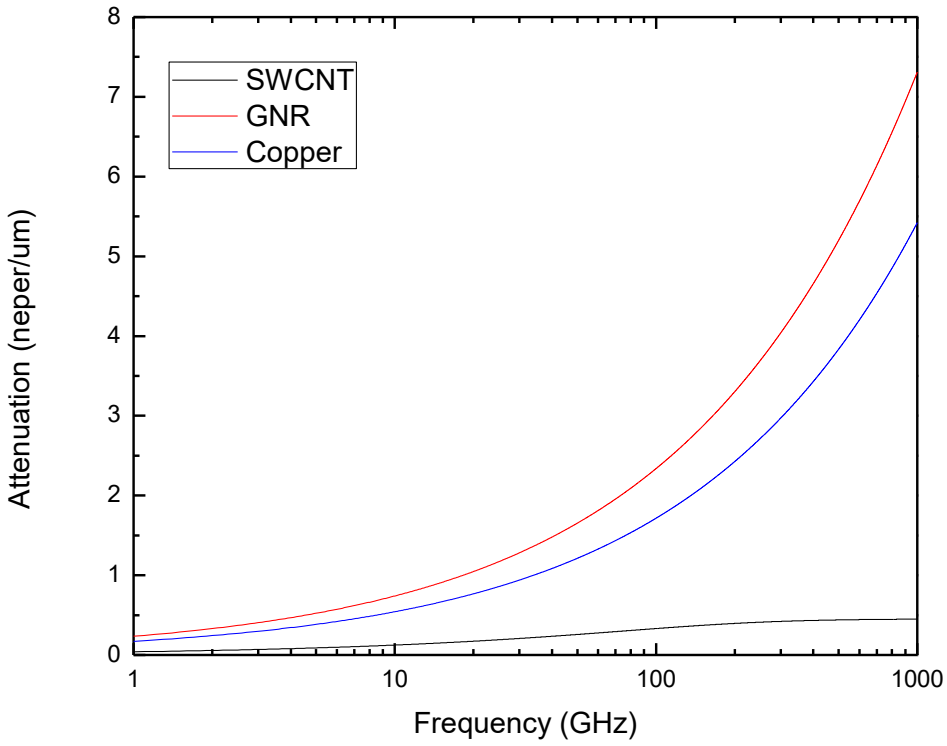

Figure 4.1: The relation between frequency and attenuation

The attenuation versus frequency characteristic of a circuit is the amount of loss through the circuit as a function of frequency. The function is shown with the amplitude in neper per meter

relative to a certain level on the vertical scale and the frequency on the horizontal scale. The figure 4.1 illustrates that when the range of frequency increases, the attenuation rate increases gradually. Initially the rate of attenuation is very low for all GNR,SWCNT and Cu. Attenuation rate is almost constantly low for SWCNT. But the attenuation rate of both GNR and copper is almost parallelly increases.The loss of GNR is greater than the loss of Cu. Here we get that the SWCNT is better to use than both GNR and Cu.

4.2 Phase Constant

Phase constant is the imaginary component of the propagation constant for a plane wave. It represents the change in phase per unit length along the path travelled by the wave at any instant and is equal to real part of the angular wavenumber of the wave. The unit of phase constant is radians per unit length [2].

$$\boldsymbol{\beta = \frac{1}{\sqrt{2}} \left[\sqrt{\omega^4 L^2 C^2 + \omega^2 R^2 C^2} + \omega^2 LC\right]^{\frac{1}{2}}} \quad \textbf{..... (4.2)}$$

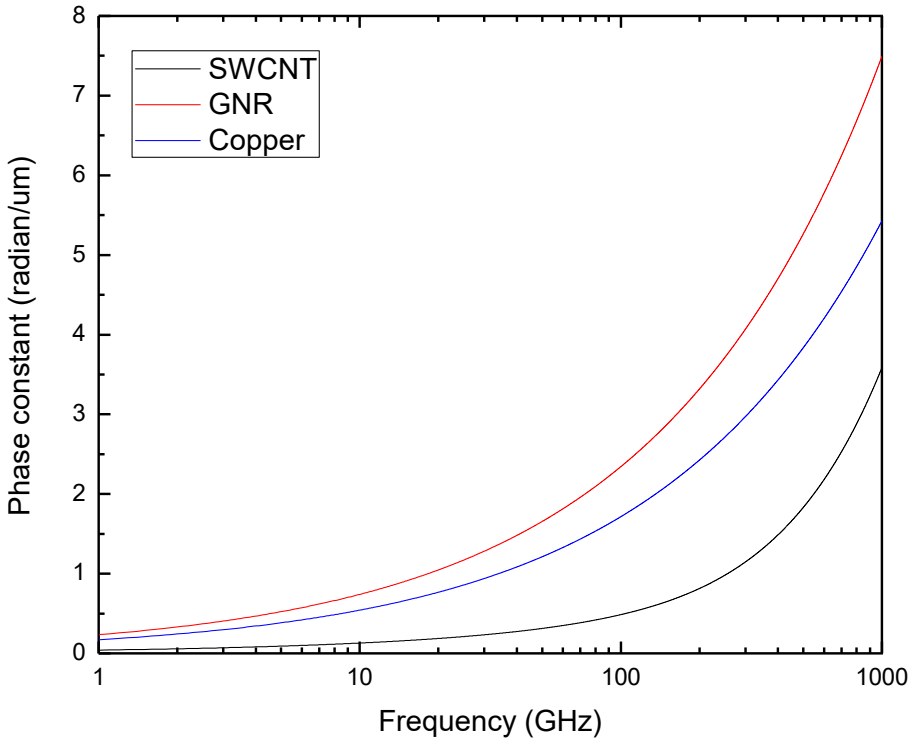

Figure 4.2: The relation between frequency and phase constant

In case of phase constant versus frequency, the graph is like a high pass. The phase constant of SWCNT increases with low amount than GNR and Cu. Phase constant of GNR is greater than the Cu.

4.3 Phase velocity

The **phase velocity** of a wave is the rate at which the phase of the wave propagates in space. This is the velocity at which the phase of any one frequency component of the wave travels. For such a component, any given phase of the wave will appear to travel at the phase velocity[3]. The phase velocity is given in terms of the angular frequency (ω) and phase constant (β) as

$$v_p = \frac{\omega}{\beta} \qquad \text{.....(4.3)}$$

$$= \frac{2.\pi.f}{\frac{1}{\sqrt{2}}\left[\sqrt{\omega^4L^2C^2+\omega^2R^2C^2}+\omega^2LC\right]^{\frac{1}{2}}}$$

$$= \frac{\sqrt{2}}{\left[\{L^2C^2+\left(\frac{RC}{\omega}\right)^2\}\text{^}(1/2)+LC\right]^{\frac{1}{2}}} \qquad \text{.....(4.4)}$$

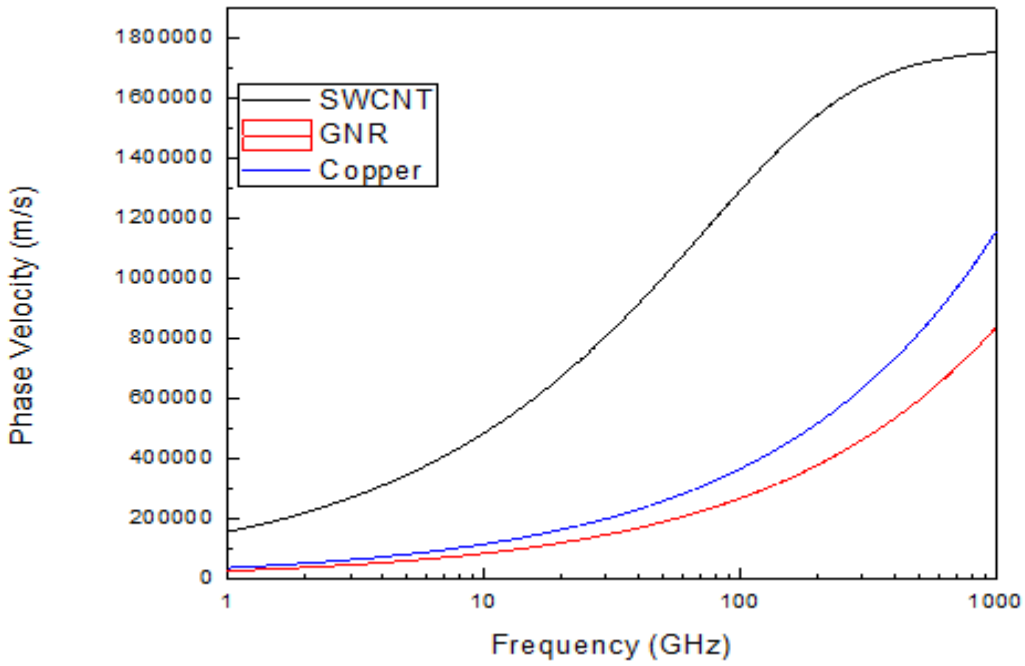

Figure 4.3: Dependency of phase constant on frequency

The graph shows that the phase velocity of GNR is very low. The Cu's phase velocity is better than GNR. The phase velocity of SWCNT is much better than both GNR and Cu.

4.4 Group velocity

The group velocity of a wave is the velocity with which the overall shape of the waves' amplitudes propagates through space. The group velocity v_g is defined by the equation below :

$V_g = \frac{d\beta}{d\omega}$ **…….(4.5)**

$= \frac{1}{2}.\frac{1}{\sqrt{2}} \left[\sqrt{\omega^4L^2C^2 + \omega^2R^2C^2} + \omega^2LC\right]^{-\frac{1}{2}} \frac{d}{d\omega} \left[\sqrt{\omega^4L^2C^2 + \omega^2R^2C^2} + \omega^2LC\right]$ **…….(4.6)**

$= = \frac{1}{2}.\frac{1}{\sqrt{2}} \left[\sqrt{\omega^4L^2C^2 + \omega^2R^2C^2} + \omega^2LC\right]^{-\frac{1}{2}} . \gamma$ **……..(4.7)**

Let $\gamma = \frac{d}{d\omega} \left[\sqrt{\omega^4L^2C^2 + \omega^2R^2C^2} + \omega^2LC\right]$

$= \frac{d}{d\omega} [\sqrt{\omega^4L^2C^2 + \omega^2R^2C^2}] + \frac{d}{d\omega} (\omega^2LC\ )$

$= \frac{1}{2}\ (\omega^4L^2C^2 + \omega^2R^2C^2\ )^{-\frac{1}{2}}\ \frac{d}{d\omega}\ (\omega^4L^2C^2 + \omega^2R^2C^2\ ) + 2\omega\ .\ \text{LC}$

$= \frac{1}{2}\ (\omega^4L^2C^2 + \omega^2R^2C^2\ )^{-\frac{1}{2}} .[\ 4\ \omega^3L^2C^2 + 2\ \omega R^2C^2] + 2\omega LC$

$= \frac{1}{2}\ \frac{4\ \omega^3L^2C^2 + 2\ \omega R^2C^2}{\sqrt{\omega^4L^2C^2 + \omega^2R^2C^2}} + 2\omega LC$ **…….(4.8)**

Now substituting (4.8) to (4.7)

$V_g = \frac{d\beta}{d\omega} = \frac{1}{2\sqrt{2}[\sqrt{\omega^4L^2C^2 + \omega^2R^2C^2} + \omega^2LC]^{\frac{1}{2}}} + [\ \frac{1}{2}\ \frac{4\ \omega^3L^2C^2 + 2\ \omega R^2C^2}{\sqrt{\omega^4L^2C^2 + \omega^2R^2C^2}} + 2\omega LC\ ]$

$= \frac{4\sqrt{2}(\sqrt{\omega^4L^2C^2 + \omega^2R^2C^2} + \omega^2LC)\sqrt{\omega^4L^2C^2 + \omega^2R^2C^2}}{3\omega^3L^2C^2 + 2\omega R^2C^2 + 4\omega LC\sqrt{\omega^4L^2C^2 + \omega^2R^2C^2}}$

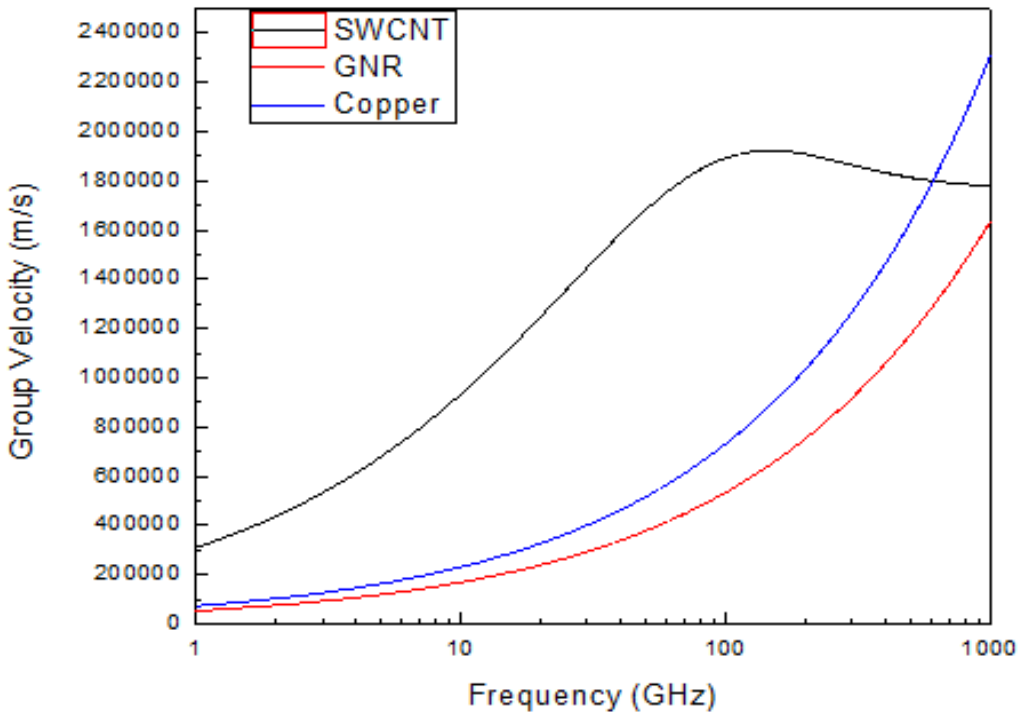

Figure 4.4: Dependency of group velocity on different frequencies

The figure 4.4 shows that the group velocity of SWCNT is better than GNR and Cu. The performance of GNR is very low and the performance of Cu is better than GNR.

Reference

1. https://en.wikipedia.org/wiki/Attenuation [Update on 18.4.2016 GMT6+]

2. https://en.wikipedia.org/wiki/Propagation_constant [Update on 18.4.2016 GMT6+]

3. https://en.wikipedia.org/wiki/Phase_velocity [Update on 18.4.2016 GMT6+]

4. https://en.wikipedia.org/wiki/Group_velocity [Update on 18.4.2016 GMT6+]

Chapter 05

Summary

In our work we have analyzed the properties of GNR. Then we compared the electromagnetic wave characteristics performance of it with the SWCNT and Copper. Our target was by comparing the 3 kinds of materials is to find out which material offers better performance in nano-scale and in higher frequencies. SWCNT has shown lowest attenuation and maximum group and phase velocity among the 3 materials. In lower frequencies SWCNT has shown better performance so it should be used in interconnect with lower frequency. In higher frequency range copper has better group velocity so it is a better choice for interconnects in higher frequency.

Appendix

1. MATLAB code for finding the relation between width and resistance.

```
clc
nl=1;
nch=2;
h=6.626*10^-34;
vf=8e5;
E0=8.854*10^-12;
u0=1.256*10^-6;
kb=1.38*10^-23;
q=1.6*10^-19;
ef=-0.21*(1.6e-19);
t=300;
ld=1e-6;
L=100e-9;
f= 1e9;
w=2*pi*f;


%Capacitance:
cq=(nl*nch*4*(q^2))/(vf*h);
ce=E0*2; %need to ask
c=(cq*ce)/ (cq+ce);
%Inductance:
lm=(u0/2);
lk= h/(4*q^2*vf*nl*nch); %need to ask
l=lm+lk;

%Resistance:
width=[1e-9 : 1e-10: 10e-9];
r=width;
vp=r;
vp2=r;
vg=r;
i=1;
rq=h/(nch*nl*2*(q^2));
syms W
for W = 1e-9 :1e-10 : 10e-9
   func=2*log(ld/W)+ 2*log(2) -2 +pi*W/ld;
   gtu2 =(8*(q^2)*(W^2)*kb*t)*func*[(log(2*cosh(ef/(2*kb*t))))];

   gtd=L*(h^2)*vf;
   gtot2 = gtu2/gtd;

   rtot2 = 1/gtot2;
```

```
   r(i)= rq+rtot2;
     i=i+1;
end
figure (01)
plot (width,r,'r')
xlabel('Width of GNR,W')
ylabel('Resistance of GNR')
title ('Relation between width vs resistance of GNR')
grid on
```

2. MATLAB code for finding the relation between both width and attenuation and width and propagation constant :

```
clc
nl=1;
nch=2;
h=6.626*10^-34;
vf=8e5;
E0=8.854*10^-12;
u0=1.256*10^-6;
kb=1.38*10^-23;
q=1.6*10^-19;
ef=-0.21*(1.6e-19);
t=300;
ld=1e-6;
L=100e-9;
f= 1e9;
w=2*pi*f;


%Capacitance:
cq=(nl*nch*4*(q^2))/(vf*h);
ce=E0*2; %need to ask
c=(cq*ce)/ (cq+ce);
%Inductance:
lm=(u0/2);
lk= h/(4*q^2*vf*nl*nch); %need to ask
l=lm+lk;

%Resistance:

width=[1e-9 : 1e-10: 10e-9];
r=width;
vp=r;
```

```
vp2=r;
vg=r;
i=1;
rq=h/(nch*nl*2*(q^2));
syms W

for W = 1e-9 :1e-10 : 10e-9
   func=2*log(ld/W)+ 2*log(2)+pi*W/ld;
   gtu2 =(8*(q^2)*(W^2)*kb*t)*func*[(log(2*cosh(ef/(2*kb*t))))];

   gtd=L*(h^2)*vf;
   gtot2 = gtu2/gtd;

   rtot2 = 1/gtot2;

   r(i)= rq+rtot2;
     i=i+1;
end



%Finding the value of alfa:
a= w^2*l*c ;
alfa = 0.7071 .* [-a + ((r.*w *c).^2 + (w^2 *l*c)^2).^0.5 ].^0.5 ;

figure (01)
plot (width , alfa , 'r')
xlabel ('width')
ylabel ('Attenuation')
title('Relation between width vs attenuation')
grid on


%Finding the value of beta:
a= w^2*l*c ;
beta = 0.7071.* [a + ((r.*w*c).^2 + (w^2 *l*c)^2).^0.5 ].^0.5 ;

figure (02)
plot (width , beta , 'r')
xlabel ('width')
ylabel ('propagation constant')
title('Relation between width vs propagation constant')
grid on
```

3. MATLAB code for finding the relation between width and phase velocity and also the relation between width and group velocity:

```
clc
nl=1;
nch=2;
h=6.626*10^-34;
vf=8e5;
E0=8.854*10^-12;
u0=1.256*10^-6;
kb=1.38*10^-23;
q=1.6*10^-19;
ef=-0.21*(1.6e-19);
t=300;
ld=1e-6;
L=100e-9;
f= 1e9;
w=2*pi*f;


%Capacitance:
cq=(nl*nch*4*(q^2))/(vf*h);
ce=E0*2; %need to ask
c=(cq*ce)/ (cq+ce);
%Inductance:
lm=(u0/2);
lk= h/(4*q^2*vf*nl*nch); %need to ask
l=lm+lk;

%Resistance:
width=[1e-9 : 1e-10: 10e-9];
r=width;
vp=r;
vp2=r;
vg=r;
i=1;
rq=h/(nch*nl*2*(q^2));
syms W
for W = 1e-9 :1e-10 : 10e-9
    func=2*log(ld/W)+ 2*log(2) -2 +pi*W/ld;
    gtu2 =(8*(q^2)*(W^2)*kb*t)*func*[(log(2*cosh(ef/(2*kb*t))))];

    gtd=L*(h^2)*vf;
    gtot2 = gtu2/gtd;
```

```
    rtot2 = 1/gtot2;

    r(i)= rq+rtot2;
       i=i+1;
end

%finding Vp
u=sqrt(2);
xc=sqrt(sqrt((l^2)*(c^2)+(r.*c./w).^2) +l*c);
vp=u./xc;

%finding Vg
s=2^(-3/2);
w2=w^2;
w3=w^3;
w4=w2^2;
B=sqrt((w4*((l^2)*(c^2)))+(w2.*((r.^2).*(c^2))));
Gi=(w4*((l^2)*(c^2))+(w2.*((r.^2).*(c^2)))).^(-1/2);
n=s.*((l*c*w2+B).^(-0.5));
m=2*l*c*w+0.5.*Gi.*(4*w3*((l*c)^2)+2.*((r.*c).^2).*w);
dw=n.*m;
vg=1./dw;

figure (01)
plot (width,vp,'r')
xlabel('Width of GNR,W')
ylabel('Phase velocity')
title ('Relation between phase velocity vs width of GNR')
grid on

figure (02)
plot (width,vg,'r')
xlabel('Width of GNR,W')
ylabel('Group Velocity')
title ('Relation between group velocity vs width of GNR')
grid on
```